Inverse Kinematics of a Redundant Manipulator based on Conformal Geometry using Geometric Approach

Je Seok Kim, Jin Han Jeong and Jahng Hyon Park
[1]*Department of Automotive Engineering, Hanyang University, Seoul, Korea*

Keywords: Geometric Approach, Inverse Kinematics Analysis, Redundancy, Conformal Geometry, Joint Angles.

Abstract: This paper describes a geometrical approach for analysing the inverse kinematics of a 7 Degrees of Freedom (DOF) redundant manipulator. The geometric approach is desirable since it provides complete and simple solutions to the problem and determines the relationship between the joints and the end-effector without iterative process. This paper introduces the approach to solve kinematic solution of 7 DOF in an intuitive way using conformal geometric approach step by step. We finally present the comparison with pseudo inverse solution which is the most well-known method in redundant manipulator kinematic problem at the same simulation environment.

SCIENCE AND TECHNOLOGY PUBLICATIONS

1 INTRODUCTION

A manipulators are designed to have the Degrees of Freedom (DOF) only needed in the configuration space, but have inherent problems, e.g., it is difficult to avoid singularity or obstacles in the operating space and lack of the adaptation to changes in operating environments. Therefore, many studies are conducted on a redundant manipulator in the form of human arm with redundancy that uses remaining DOF after performing given work to perform additional work.

Generally, velocity kinematics algorithm and geometric approach are used to analyse the inverse kinematic of redundant manipulators. The velocity kinematics algorithm (Whitney 1972, Liegeois 1977, Baillieul 1985) is based on the generalized pseudo-inverse to calculate the velocity transformation from Cartesian to joint space. Pseudo-inverse of the Jacobian matrix provides a possibility to solve for approximate solutions. There is no exact velocity solution for redundant robot. It increases the possibility of singularity and causes cumulative errors due to repeated integration of the value of speed. In terms of the geometric approach, Tolani (Tolani, Goswami et al. 2000) made a geometric approach by the shape of 7-DOF manipulator into three joints of shoulder, elbow, and wrist to express the movement of human arm naturally in computer graphics, but it was difficult to express the entities such as spheres and circles in 3D spaces. This paper attempted to reanalyse the study of Tolani in conformal geometry.

Conformal geometry is a mathematical language that integrates various mathematical theories, such as Projective Geometry, Quaternion, and Lie Algebra for easy understanding and has been widely used since the 1960s when Hestenes applied geometric algebra to physics. Therefore, it is spotlighted as a new method in robotics (Hildenbrand, Zamora et al. 2008, Aristidou and Lasenby 2011), computer vision (Bayro-Corrochano, Reyes-Lozano et al. 2006, Debaecker, Benosman et al. 2008, Ishida, Meguro et al. 2013), and computer graphics (Wareham, Cameron et al. 2005, Roa, Theoktisto et al. 2011). Conformal geometry easily expresses intuitively and mathematically the geometric entities, such as spheres and circles, from geometric perspectives to allow real-time calculations. For more details on conformal geometry, refer to the paper by Hildenbrand (Hildenbrand 2012).

The inverse kinematics analysis of manipulators in conformal geometry has already been conducted by Hildenbrand (Hildenbrand, Lange et al. 2008) and Zamora (Zamora and Bayro-Corrochano 2004). They used manipulators with 5- to 6-DOF only suitable for given configuration space and the analysis was possible only with simple geometric entities. However, 7-DOF manipulator has redundancy and it is necessary to optimize cost function.

Recently, many studies are conducted about cost function in the inverse kinematics analysis of

Seok Kim J., Han Jeong J. and Hyon Park J..
Inverse Kinematics of a Redundant Manipulator based on Conformal Geometry using Geometric Approach.
DOI: 10.5220/0005535001790185
In *Proceedings of the 12th International Conference on Informatics in Control, Automation and Robotics* (ICINCO-2015), pages 179-185
ISBN: 978-989-758-122-9
Copyright © 2015 SCITEPRESS (Science and Technology Publications, Lda.)

redundant manipulators. Cost function was suggested to make a movement similar to that of human arm using redundant DOF and a method was suggested to optimize cost function by choosing repetition and manipulability(Kim, Miller et al. 2012). However, most preceded studies have not considered the dynamic properties of manipulators and can be weak against vibration caused by link or outer load in the actual behaviour of robots. This paper also studied a method to determine the position of elbow by creating and optimizing the cost function considering the dynamic properties of manipulator for the inverse kinematic analysis of redundant manipulator in conformal geometry. Additionally, it created a simulation to plan the target route for the manipulator to accurately follow the indicated route, and compared it with the velocity kinematics algorithm.

2 INVERSE KINEMATICS

In order to express the movement of end effector, the kinematics must be analysed between the joint vector and output vector. In this chapter, we present an inverse kinematics which calculates each joint angles from the configuration of the manipulator in conformal geometry.

2.1 Redundant Manipulator

Figure 1 show a kinematic model of the redundant manipulator in this paper. It consists of a series of rigid links with seven joints (θ_1, θ_2, θ_3, θ_4, θ_5, θ_6, θ_7). In order to avoid complexity, we briefly set the basis coordinate at the bottom.

Redundant manipulator

Before analysing the kinematics, the redundant manipulator were analysed for simplicity. Since the three axes adjacent to the base and three axes adjacent to the end-effector meet at one point, we assume that the kinematic model is as follows.

- The three joints (θ_1, θ_2, θ_3) adjacent to the base were assumed as the shoulder (3-DOF)
- The one joint (θ_4) at the center of the manipulator was assumed as the elbow (1-DOF)

The three joints (θ_5, θ_6, θ_7) adjacent to the end-effector were assumed as the wrist joint (3-DOF)

2.2 Redundant Degree of Freedom

For a position of the shoulder joint fixed to the base and a position of the wrist joint along with a target position and orientation of the end-effector, the

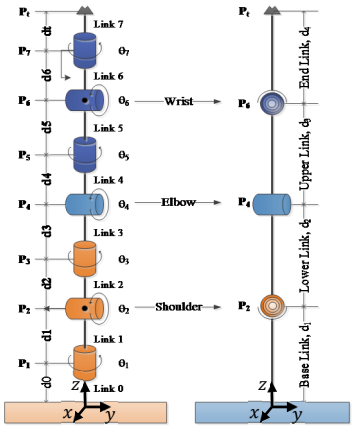

Figure 1: Redundant manipulator.

configuration of a redundant robot is fully defined if and only if the position of the elbow joint is fully specified.

As the position of shoulder is always on the z-axis of global coordinates, it can be found from the point expression of basic geometric entities in conformal geometry. Eq. (1) expresses the position of shoulder, $\mathbf{P}_2$.

$$\mathbf{P}_2 = d_1 e_3 + \frac{1}{2} d_1^2 e_\infty + e_0 \tag{1}$$

As the position of wrist is determined by the given target position and posture, it can be found using the Rigid Body Motion of fixed object in conformal geometry and is expressed by symbol, $\mathbf{P}_6$.

The position of wrist, $\mathbf{P}_6$, is defined as the point which rotates the coordinates of target position, $\mathbf{P}_t$, by target posture ($\theta_x, \theta_y, \theta_z$) and translates it by end-effector, d_4, in the direction of –z axis, as shown in Figure 2. To express the motion of fixed object, Motor, $\mathbf{M}_t$ the geometric product of Rotor, $\mathbf{R}_t$ and Translator, $\mathbf{T}_t$ is used as shown in Eq. (2):

$$\begin{aligned} \mathbf{R}_t &= \exp\left(-\frac{\theta_x}{2} e_1\right)\exp\left(-\frac{\theta_y}{2} e_2\right)\exp\left(-\frac{\theta_z}{2} e_3\right) \\ \mathbf{T}_t &= \exp\left(-\frac{d_4 e_3}{2}\right) = 1 - \frac{d_4 e_3}{2} \\ \mathbf{M}_t &= \mathbf{R}_t \mathbf{T}_t \end{aligned} \tag{2}$$

Point, $\mathbf{P}_6$, is expressed as Eq. (3) by rigid body motion of fixed object:

$$\mathbf{P}_6 = \mathbf{M}_t \mathbf{P}_t \tilde{\mathbf{M}}_t \tag{3}$$

The position of elbow, $\mathbf{P}_4$, unlike the shoulder and the wrist that are expressed by single points, is

expressed by infinite points and exists on the consistent trajectory of a circle.

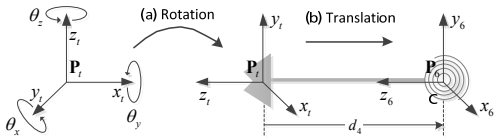

Figure 2: Wrist Point.

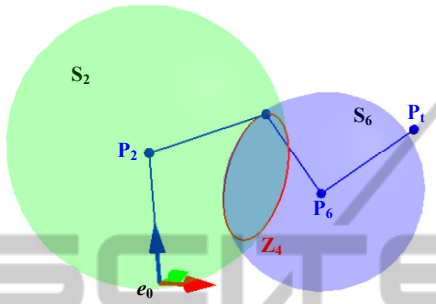

Figure 3: Intersection of spheres.

Let $\mathbf{S}_2$ be a sphere with radius d_2 and center on point $\mathbf{P}_2$, and $\mathbf{S}_6$ be a sphere with radius d_3 and center on point $\mathbf{P}_6$.

$$\mathbf{S_2} = \mathbf{P_2} - \frac{1}{2} d_2^{\,2} e_\infty \tag{4}$$

$$\mathbf{S_6} = \mathbf{P_6} - \frac{1}{2} d_3^{\,2} e_\infty \tag{5}$$

The intersection of sphere $\mathbf{S}_2$ and $\mathbf{S}_6$ is a circle $\mathbf{Z}_4$ that represents all the possible locations of point $\mathbf{P}_4$ known the positions of shoulder and wrist, as shown in Figure 3.

$$\mathbf{Z}_4 = \mathbf{S}_2 \wedge \mathbf{S}_6 \tag{6}$$

Follows a study on (D'Orangeville and Lasenby 2003), the center $\mathbf{P}_c$ and radius r_c of the circle encoded by the trivector (=circle) $\mathbf{Z}_4$ is given by

$$\begin{aligned} \mathbf{P}_c &= -\frac{\mathbf{Z}_4 e_\infty \mathbf{Z}_4}{\left(\mathbf{Z}_4 e_\infty \mathbf{Z}_4\right) \cdot e_\infty} \\ r_c &= \sqrt{-\frac{\mathbf{Z}_4^{\,2}}{(\mathbf{Z}_4 \wedge e_\infty)^2}} \end{aligned} \tag{7}$$

We have to define the redundancy angle ϕ to find the point $\mathbf{P}_4$ on the circle $\mathbf{Z}_4$. The position of the elbow joint can be expressed as a function of ϕ (Tolani, Goswami et al. 2000).

Let $\mathbf{v}$ be a normal vector of a plane containing the origin e_0, point $\mathbf{P}_2$, and point $\mathbf{P}_6$.

$$\begin{aligned} \boldsymbol{\pi}_{026} &= \left(e_0 \wedge \mathbf{P}_2 \wedge \mathbf{P}_6 \wedge e_\infty\right)^* \\ \mathbf{v} &= \frac{\boldsymbol{\pi}_{026}}{\left|\boldsymbol{\pi}_{026}\right|} \end{aligned} \tag{8}$$

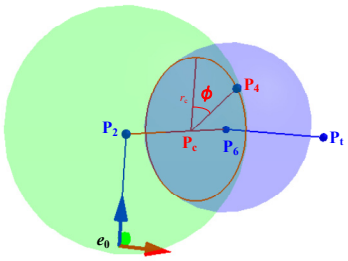

Figure 4: Elbow Circle.

A vector $\mathbf{u}$ perpendicular to the vector $\mathbf{v}$ is defined as follows:

$$\mathbf{u} = \mathbf{R}_{26} \mathbf{v} \tilde{\mathbf{R}}_{26} \tag{9}$$

where $\mathbf{R}_{26}$ represents a rotor.

$$\mathbf{R}_{26} = \exp\left(-\frac{\pi}{4}\mathbf{L}_{26}\right) \tag{10}$$

where $\mathbf{L}_{26}$ is the rotation axis, represented by a normalized bivector passing through the points $\mathbf{P}_2$ and $\mathbf{P}_6$.

Given the geometry depicted in Figure 4, the position of the elbow can be expressed as follows:

$$\mathbf{P}_4(\phi) = \mathbf{P}_c + r_c\left(\mathbf{u}\cos(\phi) + \mathbf{v}\sin(\phi)\right) \tag{11}$$

2.3 Minimization of Cost Function

This paper defined the cost function that minimizes the force imposed on joints as operators operate the manipulator considering the property that different forces are imposed on manipulators according to the location of elbow joint.

2.3.1 Euler-Lagrange Equation

Euler-Lagrange Equation is used to calculate the size of force imposed on manipulator. As Euler-Lagrange Equation uses generalized coordinates, it can be used on any coordinates that express the position of objects (Fowles and Cassiday 1999).

This paper defines generalized coordinates as the position of elbow, $\mathbf{P}_4$. Euler-Lagrange Equation is defined as follows:

$$\mathbf{F}_4 = \frac{d}{dt}\left(\frac{\partial L}{\partial \dot{\mathbf{P}}_4}\right) - \frac{\partial L}{\partial \mathbf{P}_4} \tag{12}$$

SCITEPRESS SCIENCE AND TECHNOLOGY PUBLICATIONS

Lagrangian, L, is the difference between the kinetic energy and the potential energy generated in the center of mass of each link, as follows:

$$L = T - U = \sum_{i=1}^{4} \frac{1}{2} m_i \dot{\mathbf{r}}_i^2 - \sum_{i=1}^{4} m_i g z_i \tag{13}$$

2.3.2 Center of Mass of Link

In the equation of Lagrangian, L, the center of mass of each link was converted into the function of position of elbow, $\mathbf{P}_4$, with generalized coordinates. First, the center of mass of each link was assumed as consistent bars so it can always exist on the center of link.

The center of mass of base link, $\mathbf{r}_1$, is as follows as it exists on the center of base link:

$$\mathbf{r}_1 = \frac{\mathbf{P}_2}{2} \tag{14}$$

The center of mass of lower link, $\mathbf{r}_2$, is the geometric product of Translator, $\mathbf{T}_2$, that transfers from the position of shoulder, $\mathbf{P}_2$, to the center of mass of lower link, and can be simplified as follows:

$$\begin{aligned} \mathbf{T}_2 &= 1 - \frac{\mathbf{P}_4 - \mathbf{P}_2}{2} e_\infty \\ \mathbf{r}_2 &= \mathbf{T}_2 \ \mathbf{P}_2 \ \tilde{\mathbf{T}}_2 = \mathbf{P}_2 + \frac{\mathbf{P}_4 - \mathbf{P}_2}{2} \end{aligned} \tag{15}$$

The center of mass of upper link, $\mathbf{r}_3$, can be simplified by the geometric product of Translator, $\mathbf{T}_3$, that transfers from position of wrist, $\mathbf{P}_6$, to the center of mass of lower link:

$$\begin{aligned} \mathbf{T}_3 &= 1 - \frac{\mathbf{P}_4 - \mathbf{P}_6}{2} e_\infty \\ \mathbf{r}_3 &= \mathbf{T}_3 \ \mathbf{P}_6 \ \tilde{\mathbf{T}}_3 = \mathbf{P}_6 + \frac{\mathbf{P}_4 - \mathbf{P}_6}{2} \end{aligned} \tag{16}$$

The center of mass of lower link, $\mathbf{r}_4$, is as shown below as it exists in between the position of wrist, $\mathbf{P}_6$, and the target position, $\mathbf{P}_t$:

$$\mathbf{r}_4 = \mathbf{P}_6 + \frac{\mathbf{P}_t - \mathbf{P}_6}{2} \tag{17}$$

2.3.3 Force on Elbow

When the simplified center of mass of each link is applied to Eq. (13), Lagrangian, L, is as shown below:

$$\begin{aligned} L = \frac{1}{4} & \begin{bmatrix} m_1 \dot{\mathbf{P}}_2^{\,2} + m_2 \dot{\mathbf{P}}_4^{\,2} \\ + m_3 \left(\dot{\mathbf{P}}_4 + \dot{\mathbf{P}}_6 \right)^2 + m_4 \left(\dot{\mathbf{P}}_6 + \dot{\mathbf{P}}_t \right)^2 \end{bmatrix} \\ - \frac{g}{2} & \begin{bmatrix} m_1 z_2 + m_2 \left(z_2 + z_4 \right) \\ + m_3 \left(z_4 + z_6 \right) + m_4 \left(z_6 + z_t \right) \end{bmatrix} \end{aligned} \tag{18}$$

Therefore, the force applied onto the elbow joint by Euler-Lagrange Equation is defined as follows:

$$\mathbf{F}_4 = \frac{1}{4} \left[\left(m_2 + m_3 \right) \left(\ddot{\mathbf{P}}_4 - 2g \ e_3 \right) + m_3 \ddot{\mathbf{P}}_6 \right] \tag{19}$$

2.3.4 Cost Function

The aforementioned size of force imposed on elbow varies according to the position of elbow. Therefore, the method of least squares (Haykin 1999) is used to find the point, $\mathbf{P}_{4.i}$, where the size of force imposed on elbow joint on the circle, $\mathbf{Z}_4$, becomes the smallest. The cost function is defined as the function about the size of force imposed on the elbow according to the position of elbow joint. For this purpose, Eq. (17) combines Sample Point, $\mathbf{P}_{4.i}(\phi_i)$, for the position of elbow and the size of force imposed on the elbow joint, $\|\mathbf{F}_4\|$, from Eq. (20), and expresses the equation in a quartic polynomial to make it easier to select the position of elbow. The following is defined to express the results as similarly as possible, and indicated by symbol, E:

$$\begin{aligned} & E\left[a_0, a_1, a_2, a_3, a_4 \right] \\ & = \min \sum_{i=1}^{n} \left[\|\mathbf{F}_4\| - \left(a_0 + a_1 \phi_i + a_2 \phi_i^2 + a_3 \phi_i^3 + a_4 \phi_i^4 \right) \right]^2 \end{aligned} \tag{20}$$

Here, ϕ_i is the angle that rotates the base position of elbow, $\mathbf{P}_{4.0}$, by the rotation axis, $\mathbf{L}_{26}$, and $\|\mathbf{F}_{4.i}\|$ is the size of force imposed on the position of elbow, $\mathbf{P}_{4.i}$, that is rotated by rotation angle, ϕ_i.

Cost function, E, can be partially differentiated by the factors of cost function, a_0, a_1, a_2, a_3, and a_4, as follows to find the angle, x_i, where cost function is minimized:

$$\begin{aligned} \frac{\partial E}{\partial a_0} &= -2 \sum_{i=1}^{n} \left[\|\mathbf{F}_4\| - \left(a_0 + a_1 \phi_i + a_2 \phi_i^2 + a_3 \phi_i^3 + a_4 \phi_i^4 \right) \right] \\ \frac{\partial E}{\partial a_1} &= -2 \sum_{i=1}^{n} \phi_i \left[\|\mathbf{F}_4\| - \left(a_0 + a_1 \phi_i + a_2 \phi_i^2 + a_3 \phi_i^3 + a_4 \phi_i^4 \right) \right] \\ &\vdots \\ \frac{\partial E}{\partial a_4} &= -2 \sum_{i=1}^{n} \phi_i^4 \left[\|\mathbf{F}_4\| - \left(a_0 + a_1 \phi_i + a_2 \phi_i^2 + a_3 \phi_i^3 + a_4 \phi_i^4 \right) \right] \end{aligned} \tag{21}$$

The equation equivalent to (23) is obtained by equating to 0 the right hand side of (22). This matrix form is known as Vandermonde matrix. The factor of cost function can be calculated using this matrix:

SCITEPRESS SCIENCE AND TECHNOLOGY PUBLICATIONS

$$\begin{bmatrix} a_0 \\ a_1 \\ \vdots \\ a_4 \end{bmatrix} = \begin{bmatrix} n & \sum_{i=1}^{n}\phi_i & \cdots & \sum_{i=1}^{n}\phi_i^{\,4} \\ \sum_{i=1}^{n}\phi_i & \sum_{i=1}^{n}\phi_i^{\,2} & \cdots & \sum_{i=1}^{n}\phi_i^{\,5} \\ \vdots & \vdots & \ddots & \vdots \\ \sum_{i=1}^{n}\phi_i^{\,4} & \sum_{i=1}^{n}\phi_i^{\,5} & \cdots & \sum_{i=1}^{n}\phi_i^{\,8} \end{bmatrix}^{-1} \begin{bmatrix} \sum_{i=1}^{n}\|\mathbf{F}_4\| \\ \sum_{i=1}^{n}\phi_i\|\mathbf{F}_4\| \\ \vdots \\ \sum_{i=1}^{n}\phi_i^{\,4}\|\mathbf{F}_4\| \end{bmatrix} \quad (22)$$

The value that minimizes the cost function is the point of inflection of quartic equation, so the value of this point of inflection should be found. For this purpose, the cost function of quartic equation is differentiated and the value of differentiated cubic equation is found. The value of cubic equation was found using Cardano's method (Wong and Sandler 1992). When the minimum size of force is selected among the three values, it becomes the position of value, $\mathbf{P}_4$, that becomes the smallest value.

2.4 Geometric Approach for Solving the Joint Angles

As the positions of joints are decided, the joint angle should be found. For the joint angle of manipulator, the included angle created at the intersection of two geometric entities (line, plane) can be calculated using Eq. (23). For more details, refer to the paper by (Hitzer 2013).

$$\theta = \cos^{-1}\left(\frac{\mathbf{A}^* \cdot \mathbf{B}^*}{|\mathbf{A}^*||\mathbf{B}^*|}\right) \quad (23)$$

where **A**, **B** indicates the geometric entities and only line and plane can be used as geometric entities.

However, since the range of usual principal value of the function $y=\cos^{-1}(x)$ is $0\le y\le\pi$ and the geometric entities has orientation (Cameron and Lasenby 2008), the solution for the joint angles cannot be simply calculated using the Eq. (23). Therefore, given the position of the elbow and wrist joint with respect to the base frame, we propose the solution for inverse kinematics that considers the orientation of the geometric entities.

First, all of the auxiliary planes and lines that are needed for the computation of the joint angles are calculated. We need the following:

· The plane $\boldsymbol{\pi}_{026}$ to which $\mathbf{P}_0$, $\mathbf{P}_2$ and $\mathbf{P}_6$,

$$\boldsymbol{\pi}_{026} = \mathbf{O}_1 = \left(e_0 \wedge \mathbf{P}_2 \wedge \mathbf{P}_6 \wedge e_\infty\right)^* \quad (24)$$

· The line $\mathbf{L}_{24}$ though $\mathbf{P}_2$ and $\mathbf{P}_6$,

$$\mathbf{L}_{24} = \mathbf{O}_2 = \left(\mathbf{P}_2 \wedge \mathbf{P}_4 \wedge e_\infty\right)^* \quad (25)$$

· The plane $\boldsymbol{\pi}_{246}$ to which $\mathbf{P}_2$, $\mathbf{P}_4$ and $\mathbf{P}_6$,

$$\boldsymbol{\pi}_{246} = \mathbf{O}_3 = \mathbf{P}_2 \wedge \mathbf{P}_4 \wedge \mathbf{P}_6 \wedge e_\infty \quad (26)$$

· The line $\mathbf{L}_{46}$ though $\mathbf{P}_4$ and $\mathbf{P}_6$,

$$\mathbf{L}_{46} = \mathbf{O}_4 = \mathbf{P}_4 \wedge \mathbf{P}_6 \wedge e_\infty \quad (27)$$

· The plane $\boldsymbol{\pi}_{46t}$ to which $\mathbf{P}_4$, $\mathbf{P}_6$ and $\mathbf{P}_t$,

$$\boldsymbol{\pi}_{46t} = \mathbf{O}_5 = \mathbf{P}_4 \wedge \mathbf{P}_6 \wedge \mathbf{P}_t \wedge e_\infty \quad (28)$$

· The line $\mathbf{L}_{6t}$ though $\mathbf{P}_6$ and $\mathbf{P}_t$,

$$\mathbf{L}_{6t} = \mathbf{O}_6 = \mathbf{P}_6 \wedge \mathbf{P}_t \wedge e_\infty \quad (29)$$

Now, we are able to compute solution for the first six joint angles (i=1, 2,⋯ ,6)

$$\mathbf{R}_i = \mathbf{R}_{i-1}\exp\left(-\frac{\theta_{i-1}}{2}e_{13}\right) \quad (30)$$

$$\mathbf{n}_i = \mathbf{R}_i\, e_{12}\, \tilde{\mathbf{R}}_i \quad (31)$$

For $\mathbf{O}_{i-2}$, $\mathbf{O}_i$ is the plane.

$$\mathbf{R}_i = \mathbf{R}_{i-1}\exp\left(-\frac{\theta_{i-1}}{2}e_{12}\right) \quad (32)$$

$$\mathbf{n}_i = \mathbf{R}_i\, e_{31}\, \tilde{\mathbf{R}}_i \quad (33)$$

For $\mathbf{O}_{i-2}$, $\mathbf{O}_i$ is the line.

$$\theta_i = \mathrm{sgn}\left(\left(\mathbf{O}_{i-2} \wedge \mathbf{O}_i\right)\cdot \mathbf{n}_i\right)\ \mathrm{acos}\left(\frac{\mathbf{O}_{i-2}\cdot\mathbf{O}_i}{|\mathbf{O}_{i-2}||\mathbf{O}_i|}\right) \quad (34)$$

And the solution for last joint angle is

$$\mathbf{R}_7 = \mathbf{R}_6\exp\left(-\frac{\theta_6}{2}e_{13}\right) \quad (35)$$

$$\mathbf{n}_7 = \mathbf{R}_7\, e_{12}\, \tilde{\mathbf{R}}_7 \quad (36)$$

$$\mathbf{v}_7 = \mathbf{R}_7\, e_1\, \tilde{\mathbf{R}}_7 \quad (37)$$

$$\mathbf{v}_t = \mathbf{R}_t\, e_1\, \tilde{\mathbf{R}}_t \quad (38)$$

$$\theta_7 = \mathrm{sgn}\left(\left(\mathbf{v}_7 \wedge \mathbf{v}_t\right)\cdot \mathbf{n}_7\right)\ \mathrm{acos}\left(\frac{\mathbf{v}_7\cdot\mathbf{v}_t}{|\mathbf{v}_7||\mathbf{v}_t|}\right) \quad (39)$$

3 SIMULATION

3.1 Overview of Simulation

The overall program procedure for analyzing proposed inverse kinematics algorithm of redundant manipulators in conformal geometry is shown in Figure 5.

We compared the performance of proposed inverse kinematics analysis and velocity kinematics. In this verification, we introduced a well-known method with computational time and accuracy of the solution.

SCITEPRESS SCIENCE AND TECHNOLOGY PUBLICATIONS

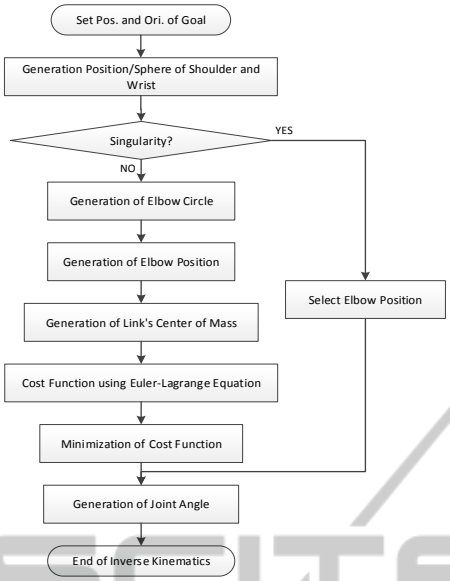

Figure 5: Inverse kinematics algorithm of redundant manipulators in conformal geometry.

3.2 Accuracy

The accuracy is the most essential evaluation points in the inverse kinematic analysis since the accuracy of the kinematic solution in a real time effects on the control performance of the manipulation. In this paper, we proved the inverse kinematic solutions by comparing joint variables (position and orientation).

We created the multiple pose of the end effector randomly and performed the test for the analysis between the proposed method and the velocity kinematics methods. We denoted the case that the manipulate works inside the valid workspace in the following table. In the case of velocity kinematics, it has highly dependence of the initial joints variables so that we set to zero.

Table 1: Comparison of accuracy.

	Velocity Kinematics	Proposed method
Pos. error [m]	7.102E-8	6.834E-14
Ori. error [rad]	2.539E-7	1.117E-13

Finally, we get the competent solution both of them. However, the velocity kinematic solution has numerical singularity region depending on the initial values.

3.3 Computation Time

The computational time plays an important role for shortening control sample time. In the same way, we tested the proposed kinematic solution with the velocity kinematic solution at the 100 sample points of the endpoint for the reasonable comparison. For the experimental setup, we constructed the system with 3.6GHz CPU and 8GB RAM with LabVIEW and performed 10 times iteratively.

Table 2: Comparison of computation time.

	Velocity Kinematics	Proposed method
Comp. time [sec]	7.320E-3	3.615E-3
Relative time	2.025	1

Table 2 represents the average time of the iterative measurements for 10 times. The computational time of the proposed method showed satisfactory performance at average # μsec comparing to the velocity kinematics. From the simulation results, we concluded that the proposed kinematic method have an advantage of real time analysis and get a unique solution precisely at the same time.

4 CONCLUSIONS

For the operating a serial manipulator, the process of solving inverse kinematics solution must be fast and accurate at the same time since the solutions are used to control the robot in a real time. Main contribution of this research is that we applied conformal geometric algebra to the redundant manipulator's kinematic solution which is intuitive and compact geometric concept but fast and accurate.

In order to compare the kinematic solution, we simulate at the same RTOS environment both pseudo inverse method and proposed method with conformal geometry. We finally concluded the kinematic solution accuracy was more satisfactory compared to previous methods and less computing time as well. This made the robot maintain stability during the motion for various operations.

ACKNOWLEDGEMENTS

This work was supported by the Research fund of the Survivability Technology Defense Research Center of the Agency for Defense Development of Korea (No. UD120019OD).

SCITEPRESS SCIENCE AND TECHNOLOGY PUBLICATIONS

REFERENCES

Aristidou, A. and J. Lasenby (2011). "FABRIK: A fast, iterative solver for the Inverse Kinematics problem." Graphical Models 73(5): 243-260.

Baillieul, J. (1985). Kinematic programming alternatives for redundant manipulators. Robotics and Automation. *Proceedings. 1985 IEEE International Conference on*, IEEE.

Bayro-Corrochano, E., L. Reyes-Lozano and J. Zamora-Esquivel (2006). "Conformal Geometric Algebra for Robotic Vision." *Journal of Mathematical Imaging and Vision 24*(1): 55-81.

Cameron, J. and J. Lasenby (2008). "Oriented conformal geometric algebra." Advances in applied Clifford algebras 18(3-4): 523-538.

D'Orangeville, C. and A. N. Lasenby (2003). Geometric algebra for physicists, *Cambridge University Press*.

Debaecker, T., R. Benosman and S.-H. Ieng (2008). Cone of view camera model using conformal geometric algebra for classic and panoramic image sensors. The 8th Workshop on Omnidirectional Vision, Camera Networks and Non-classical Cameras-OMNIVIS, Marseilles, France.

Fowles, G. R. and G. L. Cassiday (1999). Analytical mechanics, Saunders college.

Haykin, S. (1999). "Adaptive filters." Signal Processing Magazine 6.

Hildenbrand, D. (2012). Foundations of Geometric Algebra Computing, Springer.

Hildenbrand, D., H. Lange, F. Stock and A. Koch (2008). "Efficient inverse kinematics algorithm based on conformal geometric algebra using reconfigurable hardware.".

Hildenbrand, D., J. Zamora and E. Bayro-Corrochano (2008). "Inverse Kinematics Computation in Computer Graphics and Robotics Using Conformal Geometric Algebra." Advances in Applied Clifford Algebras 18(3-4): 699-713.

Hitzer, E. (2013). "Angles between subspaces." arXiv preprint arXiv:1306.1629.

Ishida, H., J.-i. Meguro, Y. Kojima and T. Naito (2013). "3D Road Boundary Detection Using Conformal Geometric Algebra." *IPSJ Transactions on Computer Vision and Applications 5*(0): 176-182.

Kim, H., L. M. Miller, N. Byl, G. Abrams and J. Rosen (2012). "Redundancy resolution of the human arm and an upper limb exoskeleton." *Biomedical Engineering, IEEE Transactions on 59*(6): 1770-1779.

Liegeois, A. (1977). "Automatic Supervisory Control of the Configuration and Behavior of Multibody Mechanisms." *Systems, Man and Cybernetics, IEEE Transactions on 7*(12): 868-871.

Roa, E., V. Theoktisto, M. Fairén and I. Navazo (2011). GPU Collision Detection in Conformal Geometric Space. V Ibero-American Symposium in Computer Graphics SIACG.

Tolani, D., A. Goswami and N. I. Badler (2000). "Real-time inverse kinematics techniques for anthropomorphic limbs." Graphical models 62(5): 353-388.

Wareham, R., J. Cameron and J. Lasenby (2005). Applications of conformal geometric algebra in computer vision and graphics. Computer Algebra and Geometric Algebra with Applications. Berlin Heidelberg, Springer: 329-349.

Whitney, D. E. (1972). "The mathematics of coordinated control of prosthetic arms and manipulators." Journal of Dynamic Systems, Measurement, and Control 94(4): 303-309.

Wong, D. S. H. and S. I. Sandler (1992). "A theoretically correct mixing rule for cubic equations of state." AIChE Journal 38(5): 671-680.

Zamora, J. and E. Bayro-Corrochano (2004). Inverse kinematics, fixation and grasping using conformal geometric algebra. Intelligent Robots and Systems, 2004. (IROS 2004). *Proceedings. 2004 IEEE/RSJ International Conference on*, IEEE.

SCITEPRESS
SCIENCE AND TECHNOLOGY PUBLICATIONS